NANO LETTERS
Letter
Cite This: Nano Lett. 2019, 19, 4442−4447
pubs.acs.org/NanoLett

Quantum Interference in a Single Perovskite Nanocrystal

Yan Lv,[†] Chunyang Yin,[†] Chunfeng Zhang,[†] William W. Yu,[‡] Xiaoyong Wang,*[,†] Yu Zhang,*[,‡] and Min Xiao*[,†,§]

[†]National Laboratory of Solid State Microstructures, School of Physics, and Collaborative Innovation Center of Advanced Microstructures, Nanjing University, Nanjing 210093, China

[‡]State Key Laboratory of Integrated Optoelectronics, and College of Electronic Science and Engineering, Jilin University, Changchun 130012, China

[§]Department of Physics, University of Arkansas, Fayetteville, Arkansas 72701, United States

Supporting Information

ABSTRACT: Coherent manipulation of the exciton wave function in a single semiconductor colloidal nanocrystal (NC) has been actively pursued in the past decades without any success, mainly due to the bothersome existence of the spectral diffusion and the photoluminescence (PL) blinking effects. Such optical deficiencies can be naturally avoided in the newly developed colloidal NCs of perovskite $CsPbI_3$, leading to the PL spectrum with a stable intensity at the single-particle level. Meanwhile, from the first-order photon-correlation measurement, a PL line width smaller than 20 μeV is estimated for the emission state of the neutral exciton in a single $CsPbI_3$ NC. Moreover, a dephasing time of about 10 ps can be extracted from the quantum interference measurement on the absorption state of the charged exciton. This stable demonstration of a coherent optical feature will advance single colloidal NCs into the quantum information regime, opening up an alternative yet prospective research direction beyond their traditional applications such as in optoelectronic devices and bioimaging.

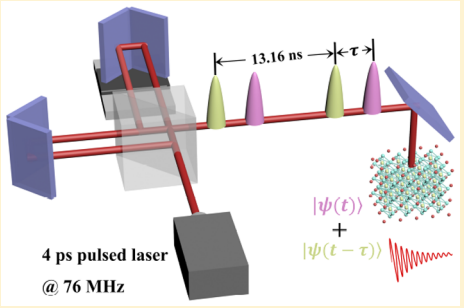

KEYWORDS: *Perovskite, nanocrystal, coherence, quantum interference*

When a quantum system is resonantly driven by two laser pulses with an increasing time delay, the wave functions generated with a correlated phase could interfere with each other to cause a population oscillation between the two-level states. This quantum interference effect, originally serving as a hallmark signature for single natural atoms,[1] was later demonstrated in the absorption state of a single epitaxial quantum dot (QD) by monitoring the photoluminescence (PL) intensity variations of its emission state.[2] The subsequent explorations of various other coherent optical properties, such as Rabi oscillations,[3] vacuum Rabi splittings,[4] and Mollow triplets,[5] have firmly pushed single epitaxial QDs to the fundamental and practical contexts of quantum information processing. In contrast, such coherent optical measurements of single colloidal nanocrystals (NCs) have never been directly implemented mainly due to their suffering from the spectral diffusion[6,7] and the PL blinking[8] effects, which would reduce the dephasing time of the absorption state and fluctuate the PL intensity of the emission state, respectively. To minimize these optical instabilities, the emission-state spectrum of a single colloidal CdSe NC had to be acquired with an integration time shorter than 100 ms by means of the photon-correlation Fourier spectroscopy (PCFS)[9] or the resonant PL excitation technique,[10] yielding a PL line width narrower than 10 μeV that could be indirectly converted to an exciton dephasing time of at least 100 ps. It is obviously challenging that a comparable dephasing time could be obtained from the quantum interference measurement normally lasting for tens of minutes, so that single colloidal NCs would truly step into the artificial-atom regime with previously unexplored coherent optical properties.

Compared to traditional metal-chalcogenide CdSe NCs that have been intensively studied for more than two decades, low-dimensional perovskites of cesium lead halide are just emerging as a novel type of colloidal NC with superior optical properties. Here, we perform PL and PL excitation measurements of single $CsPbI_3$ NCs at the cryogenic temperature of 3 K to reveal the emission and absorption states of their neutral and charged excitons, respectively. For the emission state of the neutral exciton, a PL line width less than 20 μeV can be estimated from the first-order photon-correlation measurement of a single $CsPbI_3$ NC, which is almost twice narrower than that measured for the charged exciton. For the absorption state of the charged exciton, a dephasing time of about 10 ps is extracted from the quantum interference measurement, which signifies an important step toward exploring the coherent optical properties of single colloidal NCs.

Received: March 26, 2019
Revised: May 25, 2019
Published: June 11, 2019

DOI: 10.1021/acs.nanolett.9b01237
Nano Lett. 2019, 19, 4442−4447

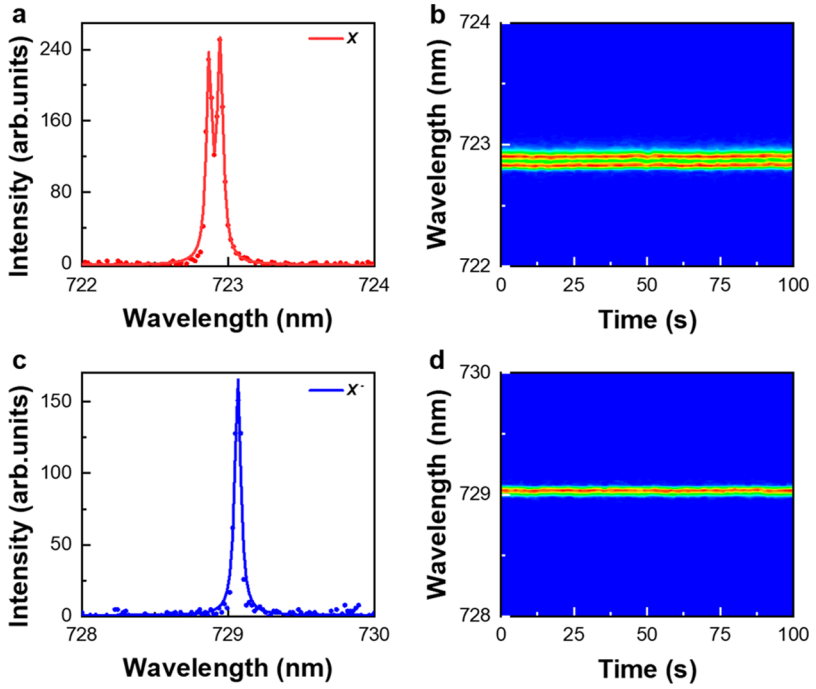

Figure 1. Emission states of single $CsPbI_3$ NCs. (a) PL spectrum and (b) time-dependent PL spectral image of the X with doublet peaks in a single $CsPbI_3$ NC. (c) PL spectrum and (d) time-dependent spectral image of the X^- with a single peak in a single $CsPbI_3$ NC. All of these PL spectra were acquired with an integration time of 1 s with unpolarized excitation and detection. The single $CsPbI_3$ NCs were excited at 590 nm with a 5.6 MHz picosecond fiber laser, and their optical signals were separated from the excitation laser by a long-pass optical filter.

The colloidal perovskite $CsPbI_3$ NCs with a cubic edge length of ~9.3 nm were chemically synthesized according to a standard procedure reported previously,[11] with their ensemble PL spectrum showing a peak wavelength of 690 nm at the room temperature. One drop of the diluted NC solution was spin-coated onto a fused silica substrate, which was later attached to the coldfinger of a helium-free cryostat operated at 3 K. The laser beam was focused by a dry objective (numerical aperture, N.A. = 0.82) onto the sample substrate, and the PL signal collected by the same objective from a single $CsPbI_3$ NC could be sent through a spectrometer to either a charge-coupled-device (CCD) camera for the PL spectral measurement or an avalanche photodiode for the PL decay measurement with a time resolution of ~200 ps. The wave plate and linear polarizer would be added to the optical path for the laser excitation and/or PL collection whenever it was necessary for the polarization-dependent measurement. To avoid any nonlinear influence of multiple excitons in a single $CsPbI_3$ NC, we normally utilized a low laser power in our optical studies corresponding to an exciton number of at most 0.1 at a given time unless otherwise specified in the text. At this exciton number and with a 5.6 MHz laser excitation, the average photon count rate measured on an avalanche photodiode for a single $CsPbI_3$ NC was $\sim 6 \times 10^2$ s^{-1}.

In Figure 1a, we plot the PL spectrum of a single $CsPbI_3$ NC excited at 590 nm with a 5.6 MHz picosecond fiber laser, where the two peaks originate from the optical emission of the neutral exciton (X) with orthogonal and linear polarizations.[11] These two peaks possess a good optical stability against the measurement time as can be seen from the PL spectral image plotted in Figure 1b with only a slight occurrence of spectral diffusion. The appearance of such a PL doublet from the X is still under active investigation and has been attributed to the electron–hole exchange interaction[11,12] or the Rashba effect[13,14] in a single perovskite NC. In Figure 1c,d, we also plot, respectively, the PL spectrum and the time-dependent PL spectral image of the charged exciton (X^-) for a single $CsPbI_3$ NC, which demonstrate a single peak due to the eliminated electron–hole exchange interaction.[11] PL transition from the X to the X^- state could be induced by an increase of the laser excitation power, which was then lowered down to leave a single $CsPbI_3$ NC permanently dwelling at the charged state. While all of the optical measurements in Figure 1 were performed at the exciton number of ~0.1, similar results are also shown in Figure S1 of the Supporting Information for single $CsPbI_3$ NCs excited at the exciton number of ~1.0. Here, we simply assume that the only type of charged exciton observed in our experiment is carrying a negative sign (X^-), but none of our main conclusions drawn below would be affected in the alternative case of a positively charged exciton (X^+). As confirmed by a previous magneto-optical measurement,[15] the photocharging effect would yield negatively charged $CsPbBr_3$ NCs at the cryogenic temperature, and this scenario can also be applied to the $CsPbI_3$ NCs since they have similar space symmetries and electronic properties.

The PL line widths of the X and X^- peaks shown in Figure 1 are mainly limited by our spectral resolution of ~100 μeV, while a precise estimation can be realized by the first-order photon-correlation measurement that has been widely applied to single epitaxial QDs.[16,17] In the following experiment, a single $CsPbI_3$ NC was excited at 632 nm by a continuous-wave He–Ne laser with the emitted photons being sent to a Michelson interferometer placed before the entrance of the spectrometer. One optical path of the interferometer was mechanically varied to generate a coarse time delay τ_c with a step resolution of 6.67 ps, while a fine time delay τ_f could be further imposed at each τ_c with a 0.2 fs step resolution. We first studied the X of a single $CsPbI_3$ NC whose PL spectral images

DOI: 10.1021/acs.nanolett.9b01237
Nano Lett. 2019, 19, 4442–4447

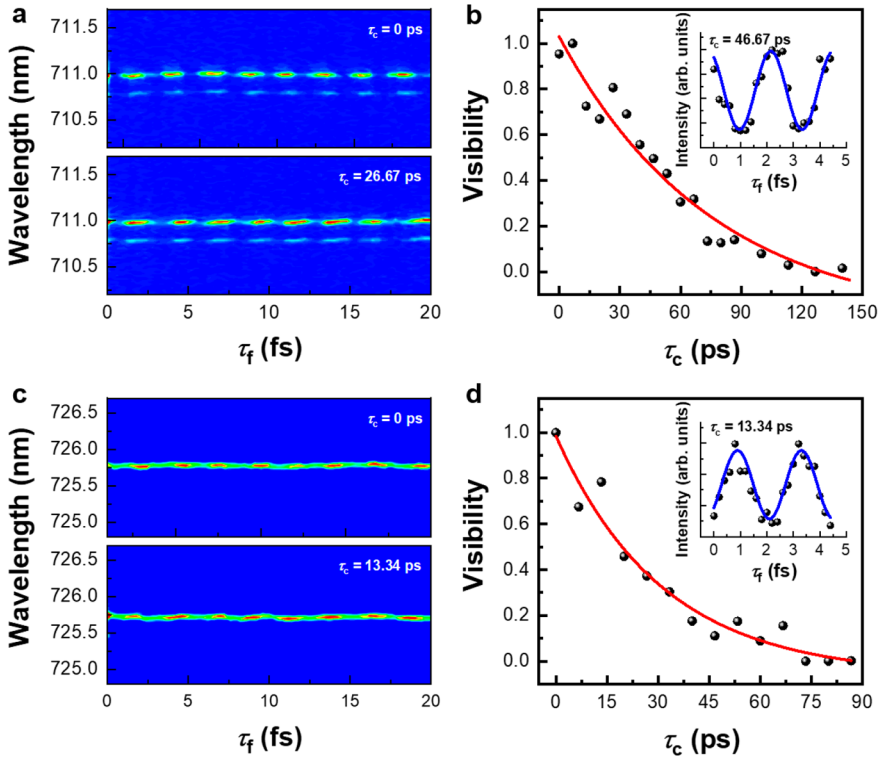

Figure 2. First-order photon-correlation measurements of single $CsPbI_3$ NCs. (a) Two-dimensional plot in the wavelength−time plane for the PL intensity oscillations of the X in a single $CsPbI_3$ NC as a function of τ_f at τ_c = 0 and 26.67 ps, respectively. The PL intensity for one of the doublet peaks was maximized through the polarized detection. (b) τ_c dependence of the X interference visibility fitted with a T_2 value of 75.86 ps. Inset: expanded view at τ_c = 46.67 ps showing the τ_f dependence of the X PL intensity oscillation. (c) Two-dimensional plot in the wavelength−time plane for the PL intensity oscillations of the X^- in a single $CsPbI_3$ NC as a function of τ_f at two τ_c positions of 0 and 13.34 ps, respectively. (d) τ_c dependence of the X^- interference visibility fitted with a T_2 value of 31.27 ps. Inset: expanded view at τ_c = 13.34 ps showing the τ_f dependence of the X^- PL intensity oscillation. The PL spectrum measured at each τ_f for the construction of the 2D plots in parts a and c was acquired with an integration time of 1 s. The single $CsPbI_3$ NCs were excited at 632 nm with a continuous-wave He−Ne laser, and their optical signals were separated from the excitation laser by a long-pass optical filter.

of the doublet peaks at two τ_c positions of 0 and 26.67 ps are plotted in Figure 2a as a function of τ_f from 0 to 20 fs. These doublet PL peaks presented very similar interferometric correlation behaviors, so we will only focus on the lower-energy one whose PL intensity was maximized through a polarized detection. In the inset of Figure 2b where τ_c was set at 46.67 ps, and τ_f was changed from 0 to 5 fs, a clear interference pattern could be observed for the PL intensity acquired in the CCD camera at each τ_f. By fitting with a sinusoidal function, the maximum and minimum PL intensities of I_{max} and I_{min} could be extracted to calculate the visibility of $(I_{max} - I_{min})/(I_{max} + I_{min})$ at a given τ_c.[17] In Figure 2b, we plot this interference visibility as a function of τ_c, which can be fitted by a single-exponential dephasing time (T_2) of 75.86 ps.

The interferometric correlation measurements were also performed on the X^- of a single $CsPbI_3$ NC, with the τ_f dependence of the PL spectral images being plotted in Figure 2c at two τ_c positions of 0 and 13.34 ps, respectively. The corresponding intensity interference is shown in the inset of Figure 2d at the τ_c position of 13.34 ps for the variation of τ_f from 0 to 5 fs. From the τ_c dependence of the interference visibility plotted in Figure 2d, a T_2 value of 31.27 ps can be extracted from a single-exponential fitting. Similar T_2 values for the X and X^- were obtained for all the other single $CsPbI_3$ NCs studied in our experiment (see Figure S2 in the Supporting Information). From the relationship of $\Gamma T_2 = h/\pi$, where h is the Planck constant, the PL line width Γ of the X (X^-) for the single $CsPbI_3$ NC studied in Figure 2a,b (Figure 2c,d) is estimated to be 17.4 (42.1) μeV. These PL line widths are obviously broader than that of ∼1.3 μeV calculated from the radiative lifetime T_1 of ∼1 ns measured for the X and X^- (see Figure S3 in the Supporting Information), implying that they are still suffering from a residual influence of the spectral diffusion effect. However, the PL line width of 17.4 μeV measured here for the X of a single $CsPbI_3$ NC has represented a significant improvement of almost 1 order of magnitude over those best values ever reported for single CdSe NCs from the time-integrated PL measurements.[6]

The existence of an ultranarrow line width in the emission state of a single $CsPbI_3$ NC should be also manifested in its absorption state, which can be probed by the PL excitation measurement. Previously, an absorption-state line width as broad as 3−4 meV was revealed from the PL excitation measurement performed on single colloidal CdSe NCs at the cryogenic temperature, where the PL blinking influence had to be intricately compensated by a special spectroscopic technique.[18] Due to the good optical stability of single $CsPbI_3$ NCs, it was easy for us to directly map their absorption states by employing a picosecond Ti:sapphire laser with a 76 MHz repetition rate. To avoid the scattered excitation light, the tunable laser was always set at an initial wavelength ∼2 nm blue-shifted relative to that of the PL peak and changed toward shorter wavelengths with a step resolution of ∼0.02 nm. In Figure 3a, we plot the PL and PL excitation spectra measured

DOI: 10.1021/acs.nanolett.9b01237
Nano Lett. 2019, 19, 4442−4447

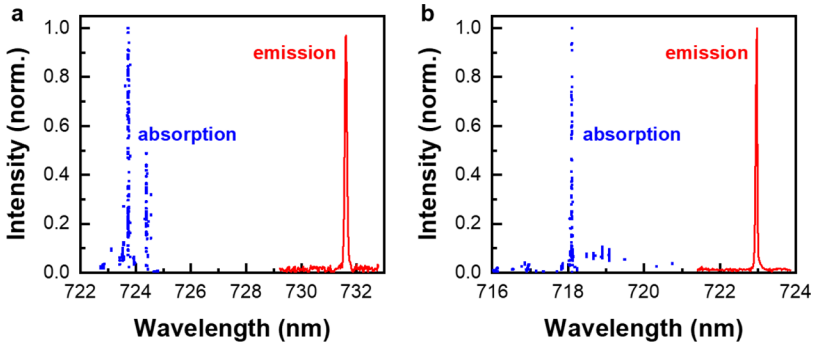

Figure 3. PL excitation measurements of single $CsPbI_3$ NCs. (a) PL and PL excitation spectra measured for the X^- of a single $CsPbI_3$ NC with two absorption states. (b) PL and PL excitation spectra measured for the X^- of a single $CsPbI_3$ NC with one absorption state. The data points for constructing the PL excitation spectrum were obtained from several scans of the tunable laser wavelength to precisely determine the peak position of the absorption state. An integration time of 1 s was employed for acquiring the PL spectrum of the emission state in the PL excitation measurement. When the single $CsPbI_3$ NCs were excited by the Ti:sapphire laser, their optical signals were separated from the excitation laser by two tunable long-pass optical filters and the 1200 g/mm grating equipped on a 0.75 m long spectrometer.

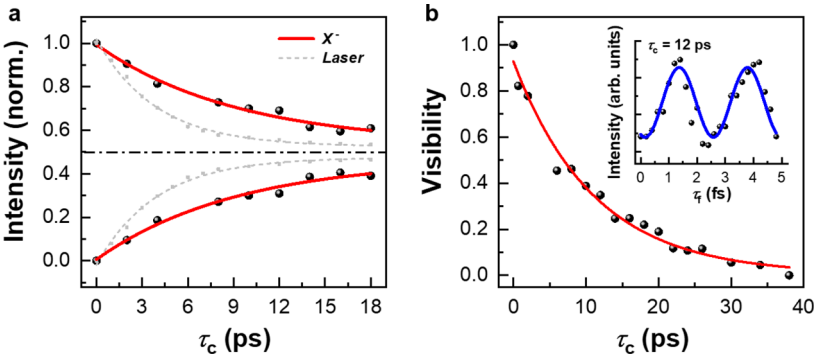

Figure 4. Quantum interference measurements of single $CsPbI_3$ NCs. (a) Maximum (top) and minimum (bottom) PL intensities measured for the X^- of a single $CsPbI_3$ NC as a function of τ_c, and each is fitted with a single-exponential function to yield a T_2 value of 9.25 ps. The gray dotted lines correspond to the autocorrelation function of the excitation laser pulses. The black dashed−dotted line marks the 0.5 position for the normalized PL intensity. (b) τ_c dependence of the X^- interference visibility measured for a single $CsPbI_3$ NC and fitted with a single-exponential function to yield a T_2 value of 11.12 ps. Inset: expanded view at τ_c = 12 ps showing the τ_f dependence of the X^- PL intensity oscillation. The PL spectrum was measured at each τ_f with an integration time of 1 s.

for the X^- of a representative $CsPbI_3$ NC, where two absorption states with resolution-limited line widths of ∼100 μeV are, respectively, resolved at higher energies of ∼16.9 and ∼19.8 meV as compared to that of the emission state. For the X^- emission state of another single $CsPbI_3$ NC shown in Figure 3b, only one absorption state shows up at a higher energy of ∼11.6 meV. Moreover, a continuous distribution of absorption states could be detected for the X^- of a single $CsPbI_3$ NC when the excitation laser was tuned even farther away from the emission state (see Figure S4a in the Supporting Information). Compared to the X^-, the PL excitation spectrum measured for the X is more complicated, displaying both discrete and clustered absorption states (see Figure S4b in the Supporting Information). Although the exact origins of these absorption states are yet to be determined in future works, their discrete existence especially in the X^- makes it possible for us to attempt the quantum interference measurement on a single $CsPbI_3$ NC.

In the next experiment, we tuned the output wavelength of the above Ti:sapphire laser to a discrete X^- absorption line of a single $CsPbI_3$ NC and sent the beam through a Michelson interferometer to generate two pulse trains with coarse (τ_c) and fine (τ_f) time delays of 2 ps and 0.2 fs step resolutions, respectively. In Figure 4a, we first plot the autocorrelation function measured for the excitation laser whose I_{max} and I_{min} change exponentially with the increasing τ_c to yield a fitted pulse width of 3.95 ps. The I_{max} and I_{min} measured for the X^- at each τ_c for a single $CsPbI_3$ NC are also presented in Figure 4a, and each was fitted by a single-exponential function of τ_c to yield a dephasing time T_2 of 9.25 ps. In the inset of Figure 4b, we plot the τ_f dependence of the PL intensity oscillation measured for a single $CsPbI_3$ NC, which serves as an example to show how I_{max} and I_{min} were obtained at a specific τ_c position of 12 ps. This sinusoidal oscillation of the PL intensity, at a time delay when the temporal overlap of the two laser pulse trains is absent, unambiguously signifies the quantum interference of the exciton wave functions in the X^- absorption state. The interference visibility of $(I_{max} - I_{min})/(I_{max} + I_{min})$ calculated at each τ_c position for this single $CsPbI_3$ NC is shown in Figure 4b, while a single-exponential fitting leads to a T_2 value of 11.12 ps. For about 10 single $CsPbI_3$ NCs studied in our experiment, an average T_2 value of 9.83 ps could be obtained with the longest and shortest T_2 values being 12.75 and 6.40 ps, respectively (see Figure S5 in the Supporting Information for two more single $CsPbI_3$ NCs). The T_2 values for the absorption state of X^- are obviously shorter than those obtained from the first-order photon-correlation measurement of the emission state, which can be naturally explained by a further reduction of the coherence time due to

DOI: 10.1021/acs.nanolett.9b01237
Nano Lett. 2019, 19, 4442−4447

the exciton relaxation process in addition to the spectral diffusion effect.

To summarize, we have performed several optical measurements on single perovskite $CsPbI_3$ NCs that are otherwise inaccessible for traditional colloidal NCs. In addition to the first-order photon-correlation and the PL excitation measurements, the quantum interference effect is successfully demonstrated for the X^- absorption state of a single $CsPbI_3$ NC with a dephasing time of ∼10 ps, which is on par with those values obtained from the earlier studies of this coherent optical phenomenon in single epitaxial QDs.[19−21] In addition to the single $CsPbI_3$ NCs studied here, it should be noted that coherent optical characterizations have also been performed very recently on ensemble $CsPbBr_2Cl$ NCs[22] and single $CsPbBr_3$ NCs.[23] In ref 22, Becker et al. applied a transient four-wave-mixing spectroscopic technique on ensemble $CsPbBr_2Cl$ NCs to obtain an exciton dephasing time of ∼24.5 ps for the emission state, corresponding to a homogeneous PL line width of ∼54 μeV. In ref 23, the single $CsPbBr_3$ NCs were still suffering from fast spectral diffusion, so Utzat et al. utilized a PCFS technique to estimate a single-NC PL line width of ∼17 μeV at the millisecond time scale, which could be transformed to an exciton coherence time of ∼78 ps for the emission state. After this pioneering work on single perovskite $CsPbBr_3$ NCs, it is naturally expected that the spectral diffusion effect should be suppressed for the generation of energy-indistinguishable single photons, and the quantum interference measurement should be realized for the long-term manipulation of the exciton coherent states. Now that the above two goals have been largely fulfilled in our current work, we are optimistic that intensive research efforts would be stimulated in future works to reveal more coherent optical properties of the newly emerged colloidal perovskite NCs so that they could be firmly advanced into the quantum-information-processing regime.

The ultranarrow PL line width of ∼23 μeV was reported for single epitaxial GaAs QDs around 1996 (ref 24), and because of its robustness against spectral diffusion, the quantum interference measurement was soon achieved in 1998 (ref 2) to serve as a starting point for the subsequent observations of various other coherent optical properties.[3−5] In great contrast, the pursuit of stable coherent optical properties from single colloidal NCs has long been impeded by the spectral diffusion effect, which is now almost completely eliminated in the $CsPbI_3$ NCs for the demonstration of the quantum interference effect. For the following coherent optical studies of single perovskite NCs, a similar research route adopted previously with single epitaxial QDs should be followed to bring these two types of important semiconductor nanostructures to the same level of the quantum-information-processing research. The quantum interference effect revealed here was from the absorption state of a single $CsPbI_3$ NC, and it is feasible borrowing previous experiences with single epitaxial QDs to obtain a longer dephasing time from the emission state by means of its resonant excitation in a microcavity to suppress the scattered laser light.[25] As to the cheap and flexible synthesis, the broad tunability across the whole visible spectrum, as well as the easy integration into different optical structures, the colloidal perovskite NCs possess obvious advantages over the traditional epitaxial QDs. It can be naturally envisioned that the colloidal perovskite NCs are capable of serving as an alternative platform to attract researchers from the epitaxial-QD community, so that their well-developed characterization tools would be applied to reproduce the old and to explore the new coherent optical properties of single perovskite NCs.

■ ASSOCIATED CONTENT

Supporting Information

The Supporting Information is available free of charge on the ACS Publications website at DOI: 10.1021/acs.nanolett.9b01237.

PL spectra obtained at high-power laser excitation, first-order photon-correlation measurements, PL decay curves, PL excitation spectra, and quantum interference measurements of single $CsPbI_3$ NCs (PDF)

■ AUTHOR INFORMATION

Corresponding Authors

*E-mail: wxiaoyong@nju.edu.cn.
*E-mail: yuzhang@jlu.edu.cn.
*E-mail: mxiao@uark.edu.

ORCID

Chunfeng Zhang: 0000-0001-9030-5606
William W. Yu: 0000-0001-5354-6718
Xiaoyong Wang: 0000-0003-1147-0051
Yu Zhang: 0000-0003-2100-621X

Notes

The authors declare no competing financial interest.

■ ACKNOWLEDGMENTS

This work is supported by the National Key R&D Program of China grant 2017YFA0303700, the National Natural Science Foundation of China grants 11574147 and 11621091, and the PAPD of Jiangsu Higher Education Institutions.

■ REFERENCES

(1) Fourkas, J. T.; Wilson, W. L.; Wäckerle, G.; Frost, A. E.; Fayer, M. D. *J. Opt. Soc. Am. B* **1989**, *6*, 1905−1910.
(2) Bonadeo, N. H.; Erland, J.; Gammon, D.; Park, D.; Katzer, D. S.; Steel, D. G. *Science* **1998**, *282*, 1473−1476.
(3) Stievater, T. H.; Li, X.; Steel, D. G.; Gammon, D.; Katzer, D. S.; Park, D.; Piermarocchi, C.; Sham, L. J. *Phys. Rev. Lett.* **2001**, *87*, 133603.
(4) Yoshie, T.; Scherer, A.; Hendrickson, J.; Khitrova, G.; Gibbs, H. M.; Rupper, G.; Ell, C.; Shchekin, O. B.; Deppe, D. G. *Nature* **2004**, *432*, 200−203.
(5) Flagg, E. B.; Muller, A.; Robertson, J. W.; Founta, S.; Deppe, D. G.; Xiao, M.; Ma, W.; Salamo, G. J.; Shih, C. K. *Nat. Phys.* **2009**, *5*, 203−207.
(6) Empedocles, S. A.; Norris, D. J.; Bawendi, M. G. *Phys. Rev. Lett.* **1996**, *77*, 3873−3876.
(7) Littleton, B. N.; Fernée, M. J.; Gómez, D. E.; Mulvaney, P.; Rubinsztein-Dunlop, H. *J. Phys. Chem. C* **2009**, *113*, 5345−5348.
(8) Nirmal, M.; Dabbousi, B. O.; Bawendi, M. G.; Macklin, J. J.; Trautman, J. K.; Harris, T. D.; Brus, L. E. *Nature* **1996**, *383*, 802−804.
(9) Coolen, L.; Brokmann, X.; Spinicelli, P.; Hermier, J.-P. *Phys. Rev. Lett.* **2008**, *100*, 027403.
(10) Biadala, L.; Louyer, Y.; Tamarat, Ph.; Lounis, B. *Phys. Rev. Lett.* **2009**, *103*, 037404.
(11) Yin, C.; Chen, L.; Song, N.; Lv, Y.; Hu, F.; Sun, C.; Yu, W. W.; Zhang, C.; Wang, X.; Zhang, Y.; Xiao, M. *Phys. Rev. Lett.* **2017**, *119*, 026401.
(12) Fu, M.; Tamarat, P.; Huang, H.; Even, J.; Rogach, A. L.; Lounis, B. *Nano Lett.* **2017**, *17*, 2895−2901.
(13) Isarov, M.; Tan, L. Z.; Bodnarchuk, M. I.; Kovalenko, M. V.; Rappe, A. M.; Lifshitz, E. *Nano Lett.* **2017**, *17*, 5020−5026.

DOI: 10.1021/acs.nanolett.9b01237
Nano Lett. 2019, 19, 4442−4447

(14) Becker, M. A.; Vaxenburg, R.; Nedelcu, G.; Sercel, P. C.; Shabaev, A.; Mehl, M. J.; Michopoulos, J. G.; Lambrakos, S. G.; Bernstein, N.; Lyons, J. L.; Stoferle, T.; Mahrt, R. F.; Kovalenko, M. V.; Norris, D. J.; Raino, G.; Efros, A. L. *Nature* **2018**, *553*, 189−193.
(15) Canneson, D.; Shornikova, E. V.; Yakovlev, D. R.; Rogge, T.; Mitioglu, A. A.; Ballottin, M. V.; Christianen, P. C. M.; Lhuillier, E.; Bayer, M.; Biadala, L. *Nano Lett.* **2017**, *17*, 6177−6183.
(16) Kammerer, C.; Cassabois, G.; Voisin, C.; Perrin, M.; Delalande, C.; Roussignol, Ph.; Gérard, J. M. *Appl. Phys. Lett.* **2002**, *81*, 2737−2739.
(17) Kuroda, T.; Sakuma, Y.; Sakoda, K.; Takemoto, K.; Usuki, T. *Appl. Phys. Lett.* **2007**, *91*, 223113.
(18) Htoon, H.; Cox, P. J.; Klimov, V. I. *Phys. Rev. Lett.* **2004**, *93*, 187402.
(19) Htoon, H.; Kulik, D.; Baklenov, O.; Holmes, A. L., Jr.; Takagahara, T.; Shih, C. K. *Phys. Rev. B: Condens. Matter Mater. Phys.* **2001**, *63*, No. 241303R.
(20) Besombes, L.; Baumberg, J. J.; Motohisa, J. *Phys. Rev. Lett.* **2003**, *90*, 257402.
(21) Toda, Y.; Sugimoto, T.; Nishioka, M.; Arakawa, Y. *Appl. Phys. Lett.* **2000**, *76*, 3887−3889.
(22) Becker, M. A.; Scarpelli, L.; Nedelcu, G.; Rainò, G.; Masia, F.; Borri, P.; Stöferle, T.; Kovalenko, M. V.; Langbein, W.; Mahrt, R. F. *Nano Lett.* **2018**, *18*, 7546−7551.
(23) Utzat, H.; Sun, W.; Kaplan, A. E. K.; Krieg, F.; Ginterseder, M.; Spokoyny, B.; Klein, N. D.; Shulenberger, K. E.; Perkinson, C. F.; Kovalenko, M. V.; Bawendi, M. G. *Science* **2019**, *363*, 1068−1072.
(24) Gammon, D.; Snow, E. S.; Shanabrook, B. V.; Katzer, D. S.; Park, D. *Science* **1996**, *273*, 87−90.
(25) Muller, A.; Flagg, E. B.; Bianucci, P.; Wang, X. Y.; Deppe, D. G.; Ma, W.; Zhang, J.; Salamo, G. J.; Xiao, M.; Shih, C. K. *Phys. Rev. Lett.* **2007**, *99*, 187402.

DOI: 10.1021/acs.nanolett.9b01237
Nano Lett. 2019, 19, 4442−4447